Nat. Hazards Earth Syst. Sci. Discuss., 2, 315–346, 2014
www.nat-hazards-earth-syst-sci-discuss.net/2/315/2014/
doi:10.5194/nhessd-2-315-2014

Natural Hazards and Earth System Sciences
Open Access
Discussions

Discharge of landslide-induced debris flows: case studies of Typhoon Morakot in southern Taiwan

J.-C. Chen and M.-R. Chuang

Dept. of Environmental and Hazards-Resistant Design, Huafan University, New Taipei, Taiwan

Received: 28 November 2013 – Accepted: 21 December 2013 – Published: 15 January 2014

Correspondence to: J.-C. Chen (jinnchyi@cc.hfu.edu.tw)

Published by Copernicus Publications on behalf of the European Geosciences Union.

Abstract

Three debris-flow gullies, the Hong-Shui-Xian, Sha-Xin-Kai, and the Xin-Kai-Dafo gullies, located in the Shinfa area of southern Taiwan were selected as case studies of the discharge of landslide-induced debris flows caused by Typhoon Morakot in 2009. The inundation characteristics of the three debris flows, such as the debris-flow volume, the deposition area, maximum flow depth, and deposition depth, were collected by field investigations and simulated using the numerical modeling software FLO-2D. The discharge coefficient c_b, defined as the ratio of the debris-flow discharge Q_{dp} to the water-flow discharge Q_{wp}, was proposed to determine Q_{dp}, and Q_{wp} was estimated by a rational equation. Then, c_b was calibrated by a comparison between the field investigation and the numerical simulation of the inundation characteristics of debris flows. Our results showed that the values of c_b range from 6 to 18, and their values are affected by the landslide ratio The empirical relationships between Q_{dp} and Q_{wp} were also presented.

1 Introduction

The debris-flow discharge is an important variable when designing debris-flow mitigation structures such as culverts, flumes, bridges, debris-flow barriers, and check dams. A debris-flow discharge can rarely be measured directly; thus, indirect methods are commonly used to estimate the discharges (Jakob, 2005). These methods include field observations, empirical methods, and numerical simulation methods. Field observations generally involve the determination of the flow velocity and cross-sectional measurements based on hydraulic formulae or channel surveys from flow superelevation, runup against obstacles, or channel characteristics (Chow, 1959; Hungr et al., 1984; Iverson et al., 1994). A debris-flow discharge can be correlated to the debris-flow volume or watershed characteristics. A variety of empirical equations relating the debris-flow peak discharge to the debris-flow volume (Mizuyama et al., 1992; Jitousono et al.,

NHESSD
2, 315–346, 2014

1996; Rickenmann, 1999) and the debris-flow peak discharge to the watershed characteristics (Bovis and Jakob, 1999) have been proposed to estimate the discharge. Attempts have been made to correlate the water-flow discharge Q_{wp} with the debris-flow discharge Q_{dp} (Takahashi, 1991; VanDine, 1985; Chen et al., 2008). The relationship between Q_{dp} and Q_{wp} was widely used in engineering planning because Q_{wp}, which is related to the return period, can be easily determined by hydrologic analysis.

The assumed Q_{dp} is proportional to Q_{wp} and is expressed as

$$Q_{dp} = c_b Q_{wp}, \tag{1}$$

where c_b is the discharge coefficient of the debris flow. Q_{wp} is generally considered at its peak value for engineering planning and determined by a rational equation (Berti et al., 1999; Chen et al., 2008). c_b depends on the sediment-supplementation conditions. The value of c_b can be high when a watershed has a high sediment supplementation. If the water contained in a debris flow has contributions solely from direct runoff, Q_{dp} is equivalent to the sum of Q_{wp} and the sediment discharge Q_s ($Q_s = c_V Q_{dp}$, where c_V is the volumetric sediment concentration). c_b in Eq. (1) is expressed as

$$c_b = (1 - c_V)^{-1}. \tag{2a}$$

Similar to Eq. (2a), an equation for the discharge coefficient for debris flows generated from gully-bed erosion was derived by Takahashi (1991), expressed as

$$c_b = \left(1 - k_c^* c_V\right)^{-1}, \tag{2b}$$

where $k_c^* = c_*^{-1}$, and c_* is the volumetric concentration of the sediment layer on the gully bed. The value of c_V of the debris flow was generally greater than 20 %, and the maximum values of c_V observed ranged up to $0.9c_*$ (Takahashi 1991). On the basis of Eq. (2a), the minimum $c_b = 1.25$ if $c_V = 0.2$; on the basis of Eq. (2b), the maximum $c_b = 10$ if $c_V = 0.9c_*$. This implies that the maximum Q_{dp} is 10 times that of Q_{wp}, and the minimum Q_{dp} is 1.25 times that of Q_{wp}.

NHESSD
2, 315–346, 2014

The debris-flow discharge is largely dependent on factors such as the initiation mechanism (the discrete landslide point source vs. the in-channel mobilization), the amount of debris entrained and deposited in the channel, and the channel morphology (Jakob, 2005). These factors may affect the value of c_b if Eq. (1) is used to compute the debris-flow discharge. However, the value of c_b calculated by Eqs. (2a) or (2b) is valid for in-channel debris flows (debris flows triggered by the in-channel mixing of water and sediment to form a debris flow) because it does not account for point-source failure volumes. Hence, the value of c_b calculated by Eqs. (2a) or (2b) may underestimate the discharge of large landslide-induced debris flows. Owing to the lack of previous studies on the value of c_b related to the landslide-induced debris flow, three debris-flow events caused by Typhoon Morakot in the Shinfa area of southern Taiwan were selected as case studies to analyze the relationship between Q_{dp} and Q_{wp} using a numerical simulation method (the FLO-2D model). When the value of c_b with the estimated Q_{wp} is provided or when the relationship between Q_{dp} and Q_{wp} is developed, the debris-flow discharge can be determined. Knowing the debris-flow discharge is helpful for the planning of debris-flow hazard mitigation.

2 Debris flows in the Shinfa area

Debris-flow hazards and rainfall

2.1 Debris-flow hazards

In 2009, Typhoon Morakot brought extreme rainfall to southern Taiwan and caused many landslides and debris flows. The study area is located in the Shinfa village of the Liouguei District, Kaoshing city, in southern Taiwan (Fig. 1). Three landslide-induced debris-flow gullies, the Hong-Shui-Xian (HSX) gully, the Sha-Xin-Kai (SXK) gully, and the Xin-Kai-Dafo (XKD) gully in the village were selected as case studies. The three debris-flow events resulted from the majority of the landslide debris that originated up-stream and entered the main stream of a gully, where it mixed with water and became a debris flow. The debris flow eroded the sidewalls of the stream, which entrained additional material that traveled further downstream. The debris-flow volume produced by the HSX gully ranged from 600 000 to 1 000 000 m^3, reporting an average approximately 800 000 m^3 (SWCB, 2009). The deposited depth was over 5 m. The debris-flow event buried the Shin-Shan hot-spring resort, damaged seven houses, and destroyed a road approximately 700 m in length (No. 133). The SXK gully produced a debris-flow volume of 800 000 to 1 100 000 m^3, reporting an average approximately 1 000 000 m^3 (SWCB 2009), in downstream areas with a deposition depth of over 6 m in certain areas. The debris flow traveled downstream into the Shinfa village and Laolung River, where over 30 houses were buried. Tragically, the debris flow caused the death of four individuals, and 24 people were reported missing. The maximum deposition width on land approached 750 m. For the debris flow in the XKD gully, the maximum deposition width was estimated to be 290 m. Six houses were buried by the debris flow; fortunately, no injury was reported in this event.

Table 1 lists the watershed area above the fan apex (A), the landslide area in A (A_L), the ratio of A_L to A (hereafter referred to as the landslide ratio R_L), and the maximum deposition width on land for the three debris-flow gullies. These gullies have a small watershed area ($A < 35$ ha), a high landside ratio ($R_L > 25$ %), and the same geological properties. The stratification in the study area is mainly composed of a Chau-chou layer and a Changchikeng layer. The Chau-chou layer is primarily composed of slate and argillite, while the Changchikeng layer is filled with deep-grey shale and light-grey sandstone.

2.2 Rainfall

The hourly and cumulative rainfall data collected from the Shinfa rain-gauge station, which is located approximately 2 km away from the SXK gully, is shown in Fig. 2. During Typhoon Morakot, an hourly maximum rainfall of 103 mm was recorded at 6.00 p.m. on 8 August 2009 (Fig. 2). The 24 h rainfall maximum of 1200 mm occurred over a period

NHESSD
2, 315–346, 2014

lasting from 3.00 a.m. on 8 August 2009 to 3.00 a.m. on 9 August 2009. The return periods from 6 h to 48 h rainfall at the Shinfa rain-gauge station exceeded 200 yr (WRA, 1999). Debris flows in the study area subsequently occurred within the period of the 24 h rainfall maximum. The three debris flows of the HSX, SXK, and XKD gullies almost occurred at the same time during 7.00 to 9.00 p.m. on 8 August 2009. Landslides and sediments slowly began to move around 7.00 p.m. on 8 August 2009, one hour after the hourly rainfall reached its maximum. During 8.30 to 9.00 p.m. on 8 August 2009, the debris flow greatly expanded in size, flowed downstream, and buried downstream areas in sediment.

3 Method

3.1 FLO-2D model

The FLO-2D (2009) routing model is software designed for two-dimensional mathematical modeling of water movement and flowing slope processes including debris flows. The FLO-2D model has been used successfully for debris-flow simulations by many researchers (e.g., Lin et al., 2005; Tecca et al., 2007; Hsu et al., 2010; Sodnik and Mikoš, 2010), and it was used to analyze the landslide-induced debris flows on alluvial fans in this work. The FLO-2D model is physically based and takes into account the mass and momentum conservation of flows. The total friction slope S_f involved in the momentum equation of the FLO-2D model considers a combination of yield, viscous, collision, and turbulent stress components (O'Brien et al., 1993). S_f is expressed as

$$S_\mathrm{f} = \frac{\tau_\mathrm{y}}{\rho h g} + \frac{K \eta v}{8 \rho h^2 g} + \frac{n^2 v^2}{h^{4/3}}, \tag{3}$$

where τ_y and η are respectively the Bingham yield stress and viscosity, ρ is the flow (sediment and water mixture) density, g is the gravitational acceleration, h is the flow depth, v is the depth-averaged velocity, K is the laminar flow resistance coefficient,

NHESSD
2, 315–346, 2014

and n is the pseudo-Manning coefficient that accounts for both the turbulent boundary friction and the internal collision stresses. The parameters related to S_f, namely the friction parameters such as τ_y, η, k, and n in Eq. (3), and the inflow hydrograph should be determined prior to debris-flow simulation.

3.2 Simulation and analysis procedure

3.2.1 Preparation of the topographic and rainfall data and the selection of parameters

1. Topographic data: topographic input data were obtained from a Digital Elevation Model (DEM) of each analyzed watershed such as the HSX, SXK, and XKD gullies. The data had a resolution of 5 m × 5 m.

2. Rainfall data: rainfall data were collected from the Shinfa rain-gauge station. The maximum hourly rainfall data from this station were used to determine the peak water-flow discharges in our study gullies during Typhoon Morakot.

3. Parameters for simulation: the friction parameters used in this paper are described as follows:

   (a) The Bingham model parameters
   Rheological properties are very important when modeling debris flows. The rheological parameters are dependent on c_V, and they have a significant effect on the debris-flow processes and final deposition morphology (FLO-2D 2009). However, c_V in real debris flows and the rheology of the complete mixture are generally not known. In some of these applications, the Bingham model parameters (τ_y and η) were inferred from the measured rheology of samples of the fine material slurry. To determine the rheological parameters of the debris flow, soil samples with a particle diameter of less than 1 mm collected from the flow area of the HSX gully were analyzed in a laboratory

NHESSD
2, 315–346, 2014

experiment using a Brookfield viscometer (type DV-III) (Chen et al., 2013). The relationship between the shear stress and the shear strain for the soil sample at various values of c_V was analyzed. The results showed that the rheological properties of the debris-flow slurries could be described by the Bingham model. The Bingham model parameters τ_y (in dynes cm^{-2}) and η (in poise) both exponentially increased with an increase in c_V, and these quantities are expressed as

$$\tau_y = 0.459 e^{16.43 c_V}, \quad (4a)$$

$$\eta = 0.0485 e^{14.94 c_V}. \quad (4b)$$

The results computed from these equations were consistent with the bounds reported in previous studies (FLO-2D, 2009; Dai et al., 1980; Fei, 1981). Equations (4a) and (4b) were used to determine the rheological parameters for the debris-flow simulations in this study.

(b) The pseudo-Manning coefficient n

n is primarily a function of the channel or land-surface roughness, and the respective flow-resistance parameters of debris flows might additionally depend to some extent on the mechanical properties of the mixture (Rickenmann, 1999). n with a value of 0.1 is usually used to analyze the debris-flow velocity by the Manning–Strickler equation (Pierson, 1986; PWRI, 1988; Rickenmann and Zimmermann, 1993); it ($n = 0.1$) was also used to simulate debris flows using the FLO-2D model (Calligaris and Zini, 2012). Generally, coarser-grained debris flows tend to require a higher value for n than finer-grained mudflows. The value of n can be determined from a mathematical model calibrated with an observed natural event (the back-calculated method). Rickenmann et al. (2006) showed that the values of the back-calculated n varied in a limited range $n = 0.07$–0.16 for a large number of debris-flow observations. The value of n can also be determined from the FLO-2D (2009) manual, where values are suggested for different surfaces over which a debris flow moves, i.e., $n = 0.2$ was adopted for the debris-flow simulation of the Hrenovec watershed, Slovenia (Sodnik et al., 2009), and $n = 0.18$ was used in the simulation of the Dolomites, Italy (Tecca et al., 2007). In this study, the values of n were determined by referencing the FLO-2D manual and the previous studies mentioned above. The value of n for the three debris-flow gullies in the Shinfa area ranged from 0.10 to 0.20. Because the simulation results for the debris-flow inundation area were not significantly affected by the value of n in the range of 0.10 to 0.20 (Chen et al., 2013), for simplicity, $n = 0.15$ was adopted for use in this study.

(c) The resistance parameter for laminar flow k

The value of k has a wide range from 24 to 50 000. In the FLO-2D manual, a higher value of $k = 2285$ is calibrated for modeling debris flows. The selection of a higher value for k would not affect the simulations (Rickenmann et al., 2006), and the influence of the value of k on the debris-flow simulation is not significant compared to the other parameters related to the flow resistance (Hsu et al., 2010). Thus, the value of $k = 2285$ typically used in the literature (e.g., Tecca et al., 2007; Sodnik and Mikoš, 2010) was used to simulate debris flows.

3.2.2 Determination of the discharge

The debris-flow discharge was determined by Eq. (1), and c_b was calibrated by comparing the results obtained from numerical simulations to those obtained from the field investigations. The value for Q_{wp} is determined from the rational equation. This equation is probably the most used method for the design of water-flow discharges (Chow et al., 1988), and it is generally used to determine the design of water-flow discharges in a mountainous gully or debris-flow gully (Berti et al., 1999; Chen et al., 2008). The rational equation is:

$$Q_{wp} = CIA/360, \quad (5)$$

where C is the runoff coefficient, I is the maximum hourly rainfall intensity (mm h^{-1}), and A is the watershed area (ha). In the study area, the value of C ranges from 0.7 to 0.9 (SWCB, 2005), and $C = 0.8$ was used; $I = 103\,\mathrm{mm\,h^{-1}}$ was the maximum hourly rainfall observed at the Shinfa rain-gauge station during Typhoon Morakot. Q_{wp} for the HSX, SXK, and XKD gullies was estimated as $7.8\,\mathrm{m^3\,s^{-1}}$, $6.8\,\mathrm{m^3\,s^{-1}}$, and $1.9\,\mathrm{m^3\,s^{-1}}$, respectively, according to the rational equation.

3.2.3 Construction of the inflow hydrograph for debris flow

According to media reports and visits by residents, landslides and sediments slowly began to move around 7.00 p.m. on 8 August 2009. This escalated into a large and rapid debris-flow event at approximately 8.30 to 9.00 p.m. that had disastrous consequences. Thus, an inflow hydrograph with a duration of 2 h (7.00–9.00 p.m.) was used. The duration of the inflow hydrograph was divided into two stages for this study. Stage one (from 7.00 to 8.30 p.m.) was the stage in which the landslides gradually transferred material to highly viscous debris flows (with a high value of c_V), and stage two (from 8.30 to 9.00 p.m.) was the stage of general debris-flow (with a lower value of c_V compared to stage one) formation. The ranges of c_V used for the two stages were obtained from reference values in the FLO-2D user's manual. Stage one used $c_V = 0.55$–0.65 for landslides or highly viscous debris flows, and stage two used $c_V = 0.48$–0.55 for general debris flows.

Because debris flows move for a short duration, the inflow hydrograph used in this study was assumed to be rectangular in shape with a duration of 2 h, as shown in Fig. 3. The benefits for using a rectangular hydrograph shape are the simple shape itself and the ease in which the relationship between Q_{dp} and Q_{wp} may be discussed or developed. If the inflow hydrograph followed the shape in Fig. 3, c_b can be computed by $c_b = V/(Q_{wp}t)$, where V is the debris-flow volume, and t is discharge duration. V is highly uncertain, and it is difficult to estimate exactly. The possible values of c_b can be determined using the ranges of V, Q_{wp} (as listed in Table 1), and t (= 2 h). The estimated c_b ranged from 11 to 18 for the HSX gully, 16 to 23 for the SXK gully, and 4 to 7 for the XKD gullies. On the basis of the estimated c_b ranges, the values of c_b were calibrated by comparing the results obtained from numerical simulations to those obtained from the field investigation.

c_V is an important factor related to the variation of the velocity of a debris flow, especially for Q_{dp} in the applied inflow hydrograph in this study, which was assumed to be constant. An inflow hydrograph with two stages of c_V values is helpful to reflect the phenomena observed in the field, which roughly indicated two stages of velocity for the landslide-induced debris flow, and it can be used to match some of the information related to the travel time of the debris flow from the field investigations. However, the real values of c_V are unknown and require calibration by comparing the inundation characteristics of a debris flow from numerical simulation to those from field investigations. The collected data from the field include the debris-flow volume, inundated area, depths (maximum flow depth, deposition depth), and flow velocity or the travel time of debris flow. Owing to lack of observation data for the velocity, some information related to the travel time of the debris flow were collected.

3.2.4 Debris-flow simulations and parameter calibration

Because debris flows often impact downstream areas where the debris is ultimately deposited, modeling the deposition area of the debris flow was the primary aim of this study. The procedures used for determining the deposition area of the debris flow and the calibration parameters (c_b and c_V) are described as follows:

1. Determine the location of the debris-flow fan apex such as the mouth of the valley or the area downstream of the topographic apex. The location of the fan apex for the debris-flow gully was obtained from a topographical map and field investigations.

2. Assume a value for c_b (as discussed in Sect. 3.2.3 or in Table 1) and a set of values for c_V (c_V = 0.55–0.65 for stage one and c_V = 0.48–0.55 for stage two) for

determining the inflow hydrograph, as indicated in Fig. 3. Input the inflow hydrograph at the debris-flow fan apex and the various friction parameters such as τ_y (Eq. 4a), η (Eq. 4b), k (= 2285), and n (= 0.15).

The inundation characteristics of a debris-flow gully was then computed via FLO-2D simulations. The results of the FLO-2D simulations were compared to the field conditions in terms of the travel time of the debris flow, the flow depth, the deposition depth, and the deposition area. If the simulated results were not in agreement with the field conditions, the inflow conditions (i.e., c_b and c_V) were adjusted until the simulated results were similar to the conditions observed in the field investigation.

4 Results

4.1 Calibrated parameters

The travel times, the deposition areas, and flow depths for the three debris-flow gullies were collected to calibrate c_b and c_V of the debris flows. Some information related to the travel time of the debris flow include a small percent of the mass or sediment that slowly flowed and blocked the road (No. 133) at 7.00–8.00 p.m. on 8 August 2009, and the debris flow rapidly inundated the downstream area and affected houses or buildings at 8.30–9.00 p.m. on 8 August 2009 (it could have attained the maximum velocity in this period).

The deposition area of the debris flows were identified through the interpretation of aerial photographs, satellite images, and field investigations. The collected flow depths in the field include the final depth (FD) (the depth of the debris-flow stoppage) and the maximum flow depth (MD). The MD was obtained according to the flow track left on buildings. The sediments left on buildings after a debris flow, e.g., the height of buildings buried by sediment, can help us to determine the FD in the field.

4.1.1 HSX gully

Figure 4 shows the results of the deposition area from the numerical simulation using the inflow hydrograph with $c_b = 14$, where the values of c_V for stages one and two were 0.64 and 0.55, respectively. The simulated results and field investigation show that part of the deposited sediment caused by the HSX debris flow flows into the Laolung River. The actual deposition area into the Laolung River was not able to be obtained from the field investigation because it was destroyed by flooding of the Laolung River. Thus, the deposition area on land from the field investigation was used for comparison with the numerical simulation. Figure 4 shows that the deposition area on land from the simulation was close to that observed during the field investigation. From the deposition area, the MD and FD of the debris flow in the field were collected. Figure 5 shows the MD and FD for the simulation and field investigation for the HSX gully. The MD and FD from the simulation are almost in agreement with those from the field investigation. The simulated results also show that the debris flow rapidly inundated the downstream area at 8.30–9.00 p.m. on 8 August 2009 with a maximum velocity of $4.2\,\mathrm{m\,s^{-1}}$. The maximum deposition depth in the debris-flow inundated area was greater than 6 m. The computed debris-flow volume from the numerical simulation is around $790\,000\,\mathrm{m^3}$, which is close to the value of approximately $800\,000\,\mathrm{m^3}$ estimated by SWCB (2009).

4.1.2 SXK and XKD gullies

Following the same procedure as in the analysis of the HSX gully, the calibrated values of the inflow hydrograph were $c_b = 18$, $c_V = 0.64$ for stage one, and $c_V = 0.50$ for stage two for the SXK gully; and $c_b = 6$, $c_V = 0.65$ for stage one, and $c_V = 0.55$ for stage two for the XKD gully. Table 2 summarizes the calibrated parameters used for the debris-flow simulations of the three case studies of the Shinfa area. With the calibrated values, Fig. 6 shows that the deposition areas of the SXK and XKD gullies from the simulations are similar to those from the field investigations. Figures 7 and 8 show the results for the MD and FD for the simulations and field investigations for SXK and XKD gullies,

NHESSD
2, 315–346, 2014

respectively. The MD and FD from the simulations are almost in agreement with those from the field investigations.

The simulated results also show that two debris flows inundated downstream areas with houses and buildings at 8.30–9.00 p.m. on 8 August 2009, which is rough agreement with information from the local populace. The SXK debris flow attained a maximum velocity of 6.6 $m\,s^{-1}$, and the XKD debris flow attained a maximum velocity of 2.1 $m\,s^{-1}$. The higher velocity of the SXK debris flow caused over 30 houses to be buried, the deaths of four people, and 24 missing people. Compared to the SXK debris flow, the damage caused by the XKD debris flow was slightly lower owing to the lower velocity of the XKD debris flow. The major building (Great Buddha in shape) in the XKD gully was nearly complete, and no injuries were reported in this event. The simulated debris-flow volumes V were around 880 000 m^3 for the SXK gully and 82 000 m^3 for XKD gully.

4.2 Relationship between the debris-flow discharge and the water-flow discharge

According to the calibrated values of c_b (in the range from 6 to 18) in Table 2 for the three gullies in the Shinfa area, Q_{dp} corresponding to the peak water-flow discharge Q_{wp} was calculated from Eq. (1) and is plotted in Fig. 9. Data for Q_{dp} vs. Q_{wp} was also used to compare with the data from previous studies. Table 3 lists the sources or methods for the determination of Q_{dp} and Q_{wp} from previous studies. The data from previous studies include the field observation data on debris flows in the Jiangjia Gully in China (Wu et al., 1990), field experiments on debris flows at the Chemolgan test site in Kazakhstan (Rickenmann et al., 2003), and the estimated peak debris-flow discharges in the Howe Sound in British Columbia (VanDine, 1985) and in the Dolomites mountains in Northeastern Italy (Berti et al., 1999). Data related to the maximum debris-flow discharge and the 100 yr-design water discharge of the Predelica torrent in the Log pod Mangartom village, Slovenia in November 2000 (Četina et al., 2006; Mikoš et al., 2007) were also collected. Figure 9 shows that Q_{dp} increases with increasing Q_{wp}. The upper and lower bounds for the relationships for Q_{dp} associated with Q_{wp} are approximately expressed by

$$Q_{dp} = 40Q_{wp}, \quad \text{for the upper bound,} \tag{6}$$

$$Q_{dp} = 5Q_{wp}, \quad \text{for the lower bound.} \tag{7}$$

These equations imply that the values of c_b range from 5 to 40. All data in this work (labelled 1, 2, and 3 in Fig. 9) agreed with the ranges from previous studies. The upper bound for Q_{dp} vs. Q_{wp} in our case studies is close to $Q_{dp} = 20Q_{wp}$.

4.3 Relationship between the discharge coefficient and the landslide ratio

The values of c_b at different areas may be different owing to different hydrogeological conditions such as rainfall, watershed area, landslide area, and topographical and geological properties. The three debris-flow gullies in this study have similar rainfall and geological conditions. Figure 10 shows that the values of c_b increase with an increase in R_L. This result means that c_b was affected by the large sediment supplement brought in from the landslides and increased its value. In addition to direct runoff, the water flow that initiated the debris flow likely originated from the ground water or the water contained in sediments that were brought in by the landslides. Furthermore, the water flow could have been blocked by the sediment brought in by landslides, which would have rapidly increased the water storage in the watershed. A high debris-flow discharge may have resulted when the stored water combined with sediments burst over a short period of time. A high debris-flow discharge will be reflected by a higher discharge coefficient (c_b). For gully-bed instability or erosion-induced debris flows (the in-channel debris flow), the maximum value of c_b could be as high as 10 based on the viewpoint of Takahashi (1991), while the value of c_b for high-R_L-induced debris flows (> 30 %) could exceed the bound ($c_b = 10$) proposed by Takahashi (1991), as shown in Fig. 10. This means that the value of c_b for the debris-flow type that forms from landslides is not able to be determined merely from Eqs. (2a) or (2b). The case studies on the value of c_b for landslide-induced debris flows in this work could be helpful for determining the debris-flow discharge in the engineering or planning of debris-flow hazard mitigation.

5 Conclusions

The debris-flow discharge is an important parameter for engineering planning design and evaluating the inundation area of debris flow. Because the debris-flow discharge is difficult to measure directly, a numerical simulation method was proposed to calibrate the discharge coefficient c_b of the debris flow and to determine the debris-flow discharge. Three debris-flow hazards in southern Taiwan caused by Typhoon Morakot in 2009 were selected as case studies for the discharge of landslide-induced debris flows. An inflow hydrograph assumed to be rectangular in shape and divided into two stages of sediment concentration c_V was used. The two parameters c_b and c_V involved in the inflow hydrograph were calibrated and presented. The calibrated values of c_b for the three gullies ranged from 6 to 18, and they tended to increase with an increase in the landslide ratio R_L. The value of c_b for high-R_L-induced debris flows ($R_L > 30\,\%$) could exceed the bound of $c_b = 10$ for in-channel debris flows.

The empirical relationships between Q_{dp} and Q_{wp} were presented by collecting the data of Q_{dp} vs. Q_{wp} from previous studies and using the data of Q_{dp} vs. Q_{wp} in this study. Q_{dp} tends to increase with increasing Q_{wp}. The upper bound for the relationship between Q_{dp} and Q_{wp} can be approximately expressed as $Q_{dp} = 40Q_{wp}$, and the lower bound is $Q_{dp} = 5Q_{wp}$; that is, c_b ranges from 5 to 40. When c_b and Q_{wp} (estimated by a rational equation) are known, Q_{dp} is determined by Eq. (1). The empirical relationships developed in this study could be useful for determining the debris-flow discharge for engineering planning and evaluating the inundation area of a debris flow.

NHESSD
2, 315–346, 2014

Acknowledgements. The authors thank the National Science Council of Taiwan for financial support. The data were kindly provided by the Soil and Water Conservation Bureau of Taiwan, National Cheng Kung University, and J. S. Wang. The authors also appreciate C. J. Jeng, S. Y. Sun, and D. R. Su for their help in the field investigations, the handling editor K. Chang, the reviewer J. Sodnik, and two anonymous reviewers for their critical reviews and constructive comments.

References

Berti, M., Genevois, R., Simoni, A., and Tecca, P. R.: Field observation of a debris flow event in the Dolomites, Geomorphology, 29, 265–274, 1999.

Bovis, M. J. and Jakob, M.: The role of debris supply conditions in predicting debris flow activity, Earth Surf. Proc. Land., 24, 1039–1054, 1999.

Calligaris C and Zini, L.: Debris flow phenomena: a short overview?, in: Earth Sciences, edited by: Dar, I. A., InTech, 2012.

Četina, M., Rajar, R., Hojnik, T., Zakrajšek, M., Krzyk, M., and Mikoš, M.: Case study: numerical simulations of debris flow below Stože, Slovenia, J. Hydraul. Eng., 132, 121–130, 2006.

Chen, J. C., Jan, C. D., and Lee, M. S.: Reliability analysis of design discharge for mountainous gully flow, J. Hydraul. Res., 46, 835–838, 2008.

Chen, J. C., Jeng, C. J., and Chuang, M. R.: Numerical simulation for landslides induced debris flow – a case study of Hong-Shui-Xian gully in southern Taiwan, Sino-Geotechnics, 137, 40–47, 2013 (in Chinese).

Chow, V. T.: Open-Channel Hydraulics, McGraw-Hill, 1959.

Chow, V. T., Maidment, D. R., and Mays, L. W.: Applied Hydrology, McGraw-Hill, 1988.

Dai, J., Chen, W., and Zhou, B.: An experimental study of slurry transport in pipes, in: Proc. Int. Symposium on River Sedimentation, 195–204, 1980.

Fei, X. J.: Bingham yield stress of sediment water mixtures with hyperconcentration, J. Sediment. Res., 3, 19–28, 1981 (in Chinese).

FLO-2D: FLO-2D Users Manual, Ver. 2009. FLO-2D Software Inc, Nutrioso, AZ, USA, 2009.

Hsu, S. M., Chiou, L. B., Lin, G. F., Chao, C. H., Wen, H. Y., and Ku, C. Y.: Applications of simulation technique on debris-flow hazard zone delineation: a case study in Hualien County, Taiwan, Nat. Hazards Earth Syst. Sci., 10, 535–545, doi:10.5194/nhess-10-535-2010, 2010.

Hungr, O., Morgan, G. C., and Kellerhals, R.: Quantitative analysis of debris torrent hazards for design of remedial measures, Can. Geotech. J., 21, 663–677, 1984.
Iverson, R. M., LaHusen, R., Major, J. J., and Zimmerman, C. L.: Debris flow against obstacles and bends: dynamics and deposits, EOS T. Am. Geophys. Un., 75, p. 274, 1994.
Jakob, M.: Debris-flow hazards analysis, in: Debris-Flow Hazards and Related Phenomena, edited by: Jakob, M. and Hungr, O., Springer-Praxis, Chichester, UK, 411–443, 2005.
Jitousono, T., Shimokawa, E., and Tsuchiya, S.: Debris flow following the 1994 eruption with pyroclastic flows in Merapi volcano, Indonesia, J. Jap. Soc. Erosion Control Eng., 48, 109–116, 1996.
Lin, M.-L., Wang, K.-L., and Huang, J.-J.: Debris flow run off simulation and verification – case study of Chen-You-Lan Watershed, Taiwan, Nat. Hazards Earth Syst. Sci., 5, 439–445, doi:10.5194/nhess-5-439-2005, 2005.
Mizuyama, T., Kobashi, S., and Ou, G.: Prediction of debris flow peak discharge, in: Proc. Int. Symp. Interpraevent, Bern, Switzerland, Bd. 4, 99–108, 1992.
O'Brien, J. S., Julien, P. Y., and Fullerton, W. T.: Two-dimensional water flood and mudflow simulation, J. Hydraul. Eng., 119, 244–261, 1993.
Pierson, T. C.: Flow behavior of channelized debris flows, Mt. St. Helens, Washington, in: Hillslope Processes, edited by: Abraham, A. D., Allen & Unwin, Boston, 269–296, 1986.
PWRI: Technical standard for measures against debris flow (draft), Technical Memorandum of PWRI, No. 2632, Ministry of Construction, Japan, 1988.
Mikoš, M, Fazarinc, R., and Majes, B.: Delineation of risk area in Log pod Mangartom due to debris flows from the Stože landslide, Acta Geogr. Slov., 47, 171–198, 2007.
Rickenmann, D.: Empirical relationships for debris flows, Nat. Hazards, 19, 47–77, 1999.
Rickenmann, D. and Zimmermann, M.: The 1987 debris flows in Switzerland: documentation and analysis, Geomorphology, 8, 175–189, 1993.
Rickenmann, D., Weber, D., and Stepanov, B.: Erosion by debris flows in Field and laboratory experiments, in: Proceedings of the 3rd International conference on debris-flow hazards mitigation, Davos, Switzerland, edited by: Rickenmann, D. and Chen, C. L., Millpress, Rotterdam, 883–894, 2003.
Rickenmann, D., Laiglec, D., McArdell, B. W., and Hübl, J.: Comparison of 2D debris-flow simulation models with field events, Comput. Geosci., 10, 241–264, 2006.
Sodnik, J. and Mikoš, M.: Modeling of a debris flow from the Hrenovec torrential watershed above the village of Kropa, Acta Geogr. Slov., 50, 59–84, 2010.

NHESSD
2, 315–346, 2014

Discharge of landslide-induced debris flows

J.-C. Chen and M.-R. Chuang

Sodnik, J., Petje, U., and Mikoš, M.: Terrain topography and debris-flow modelling, Geod. Vestn., 53, 305–318, 2009.

SWCB: Technical Handbook of Soil and Water Conservation, Soil and Water Conservation Bureau (SWCB), Taiwan, 2005 (in Chinese).

SWCB: Disasters caused by Typhoon Morakot in Taiwan, 2009, Soil and Water Conservation Bureau (SWCB), Taiwan, 2009 (in Chinese).

Takahashi, T.: Debris Flow, IAHR Monograph, Balkema, Rotterdam, 1991.

Tecca, P. R., Genevois, R., Deganutti, A. M., and Armento, M. C.: Numerical modelling of two debris flows in the Dolomites (Northeastern Italian Alps), in: Debris-Flow Hazards Mitigation: Mechanics, Prediction, and Assessment, edited by: Chen, C. L. and Major, J. J., Millpress, the Netherlands, 179–188, 2007.

VanDine, D. F.: Debris flow and debris torrents in the Southern Canadian Cordillera, Can. Geotech. J., 22, 44–68, 1985.

Wu, J. S., Kan, Z. C., Tian, L. C., and Zhang, S. C.: Observational investigation of debris flow in the Jianglia gully, Yunnan, Science Publishing Co., 1–251, 1990 (in Chinese).

WRA (Water Resources Agency): Report on the analysis of the rainfall brought by Typhoon Morakot in Taiwan, Ministry Economic Affairs of Taiwan, 1999.

NHESSD
2, 315–346, 2014

Table 1. Hydrogeological parameters for the three debris-flow gullies in the Shinfa area.

Name of gully	A (ha)	H (m)	A_L (ha)	R_L (%)	W (m)	V ($\times 10^3$ m^3)	Q_{wp} (cms)
HSX gully	34.1	700	11.4	33.4	640	600–1000	7.8
SXK gully	29.7	225	12.1	40.7	750	800–1100	6.8
XKD gully	8.3	145	2.12	25.5	290	50–100	1.9

A = Watershed area; H = Max. elevation difference in the watershed; A_L = Landslide area in the watershed; R_L = Landslide ratio ($R_L = A_L/A$); W = Max. deposition width on land; and V = debris flow volume. Q_{wp} = Estimated peak water discharge determined by the rational equation (Eq. 5) using $C = 0.8$ and $I = 103\,\mathrm{mm\,h^{-1}}$.

NHESSD
2, 315–346, 2014

Table 2. Calibrated parameters used for debris-flow simulations of the three gullies in the Shinfa area.

Name of gully	R_L (%)	Q_{wp} (cms)	c_b	c_V at stage 1	c_V at stage 2
HSX gully	30.3	7.8	14	0.64	0.55
SXK gully	40.7	6.8	18	0.64	0.50
XKD gully	25.5	1.9	6	0.65	0.55

Note: Other parameters related to the flow resistance adopted in this study were $n = 0.15$ and $k = 2285$.

NHESSD
2, 315–346, 2014

Table 3. Summary of the estimation of the debris-flow discharge and water-flow discharge from previous studies.

Location	Q_{dp}	Q_{wp}	Source
The Chemolgan test site, Kazakhstan	Determined from field experiments on debris flows for measurements and calculations of debris-flow surges	Debris flows were artificially triggered by releasing water from a reservoir. A total of eight experiments on debris flows were carried out between 1972 and 1991. Q_{wp} was measured by controlling the inflow gate from the reservoir.	Rickenmann et al. (2003)
Jiangjia Gully, China	Determined from observation data of debris-flow surges for a debris event	Q_{wp} was determined from the hydrologic design handbook in the study area using the watershed characteristics and the rainfall intensity of the rainfall event triggering the debris flow.	Wu et al. (1990)
Gully in the Dolomites mountains, Northeastern Italy	Estimated from superelevations of lateral deposits or mudlines left by the peak discharge using a superelevation formula.	Q_{wp} was estimated using a rational equation using the watershed characteristics and rainfall intensity of the rainfall event triggering debris flow in the study area.	Berti et al. (1999)
22 creeks along Howe Sound, British Columbia	Estimated from the superelevations of lateral deposits or the mudlines left by the peak discharge using a superelevation formula.	Q_{wp} was determined by hydrologic analysis using a 200 yr water-discharge design.	Hungr et al. (1984); VanDine (1985)

Discussion Paper | Discussion Paper | Discussion Paper | Discussion Paper |

NHESSD

2, 315–346, 2014

Discharge of landslide-induced debris flows

J.-C. Chen and M.-R. Chuang

Title Page
Abstract Introduction
Conclusions References
Tables Figures
Back Close
Full Screen / Esc
Printer-friendly Version
Interactive Discussion

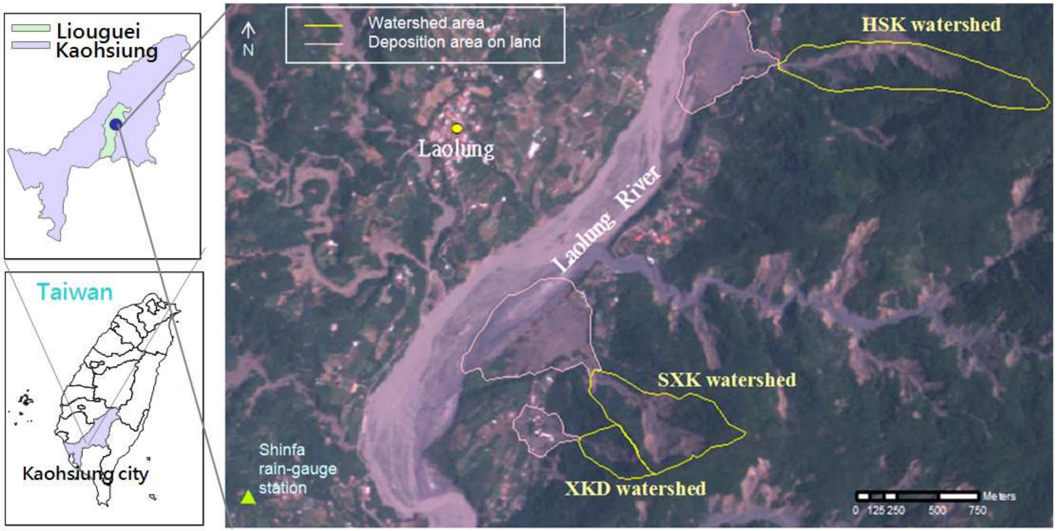

Fig. 1. Locations of the HSX, SXK, and XKD gullies and the deposition areas of the debris flows during Typhoon Morakot in 2009.

NHESSD
2, 315–346, 2014

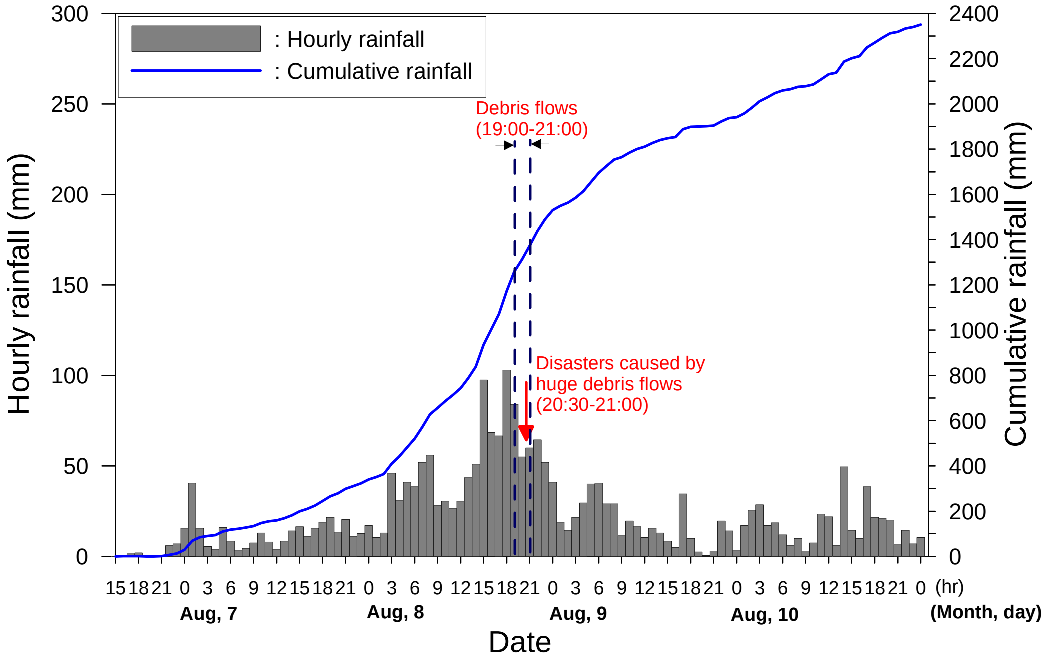

Fig. 2. Rainfall data collected from 7 August 2009 to 10 August 2009 at the Shinfa rain-gauge station and the time that a debris flow was triggered.

NHESSD
2, 315–346, 2014

Discharge of landslide-induced debris flows

J.-C. Chen and M.-R. Chuang

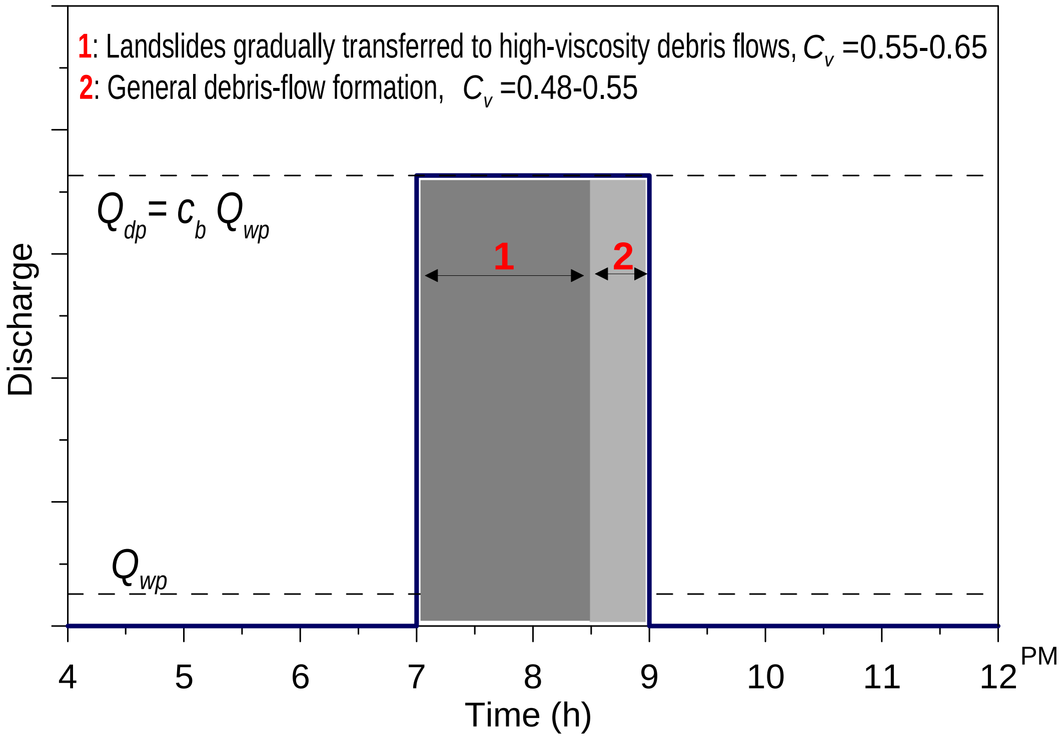

Fig. 3. Schematic of the inflow hydrograph used for this study. The hydrograph was divided into stages 1 and 2 for the simulations of debris flows.

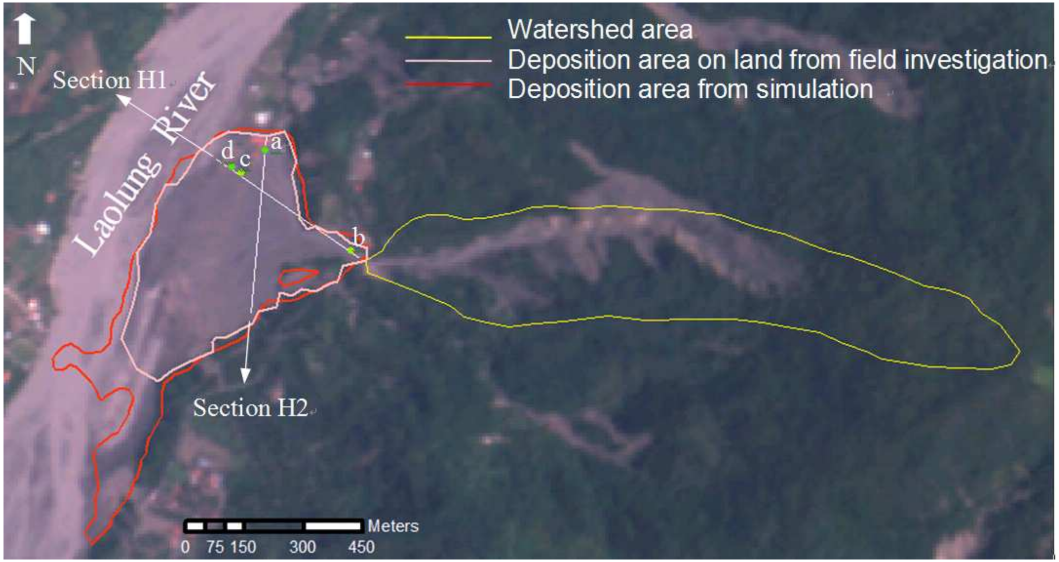

Fig. 4. Comparison of the deposition area between the simulation and the field investigation. A few flow depths are indicated by green circles collected from the field investigation of the HSX gully.

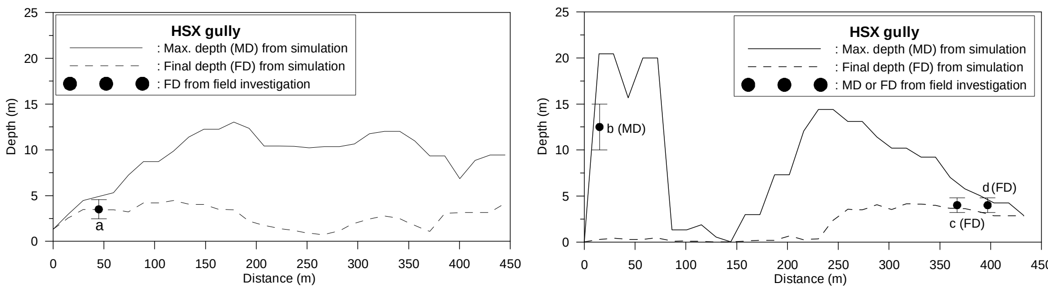

Fig. 5. Depths of the debris-flow profiles from the simulation compared to the depths from the field investigation of the HSX gully.

NHESSD
2, 315–346, 2014

Discharge of landslide-induced debris flows

J.-C. Chen and M.-R. Chuang

Title Page
Abstract | Introduction
Conclusions | References
Tables | Figures
◀ | ▶
Back | Close
Full Screen / Esc
Printer-friendly Version
Interactive Discussion

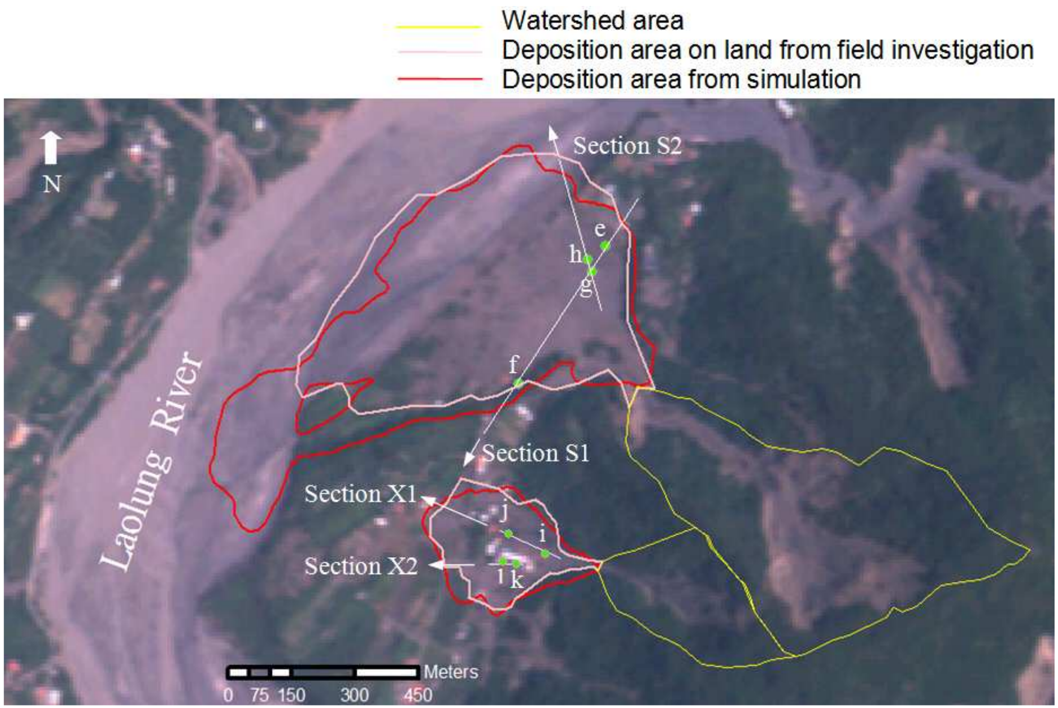

Fig. 6. Comparison of the deposition areas between the simulations and the field investigations. A few flow depths are indicated by green circles collected from the field investigations of the SXK and XKD gullies.

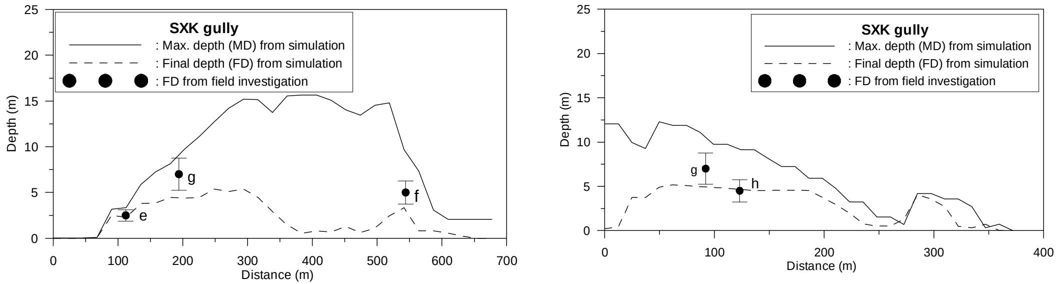

(a) section S1 (b) section S2

Fig. 7. Depths of the debris-flow profiles from the simulation compared to the depths from the field investigation of the SXK gully.

NHESSD
2, 315–346, 2014

Title Page
Abstract | Introduction
Conclusions | References
Tables | Figures
◀I | ▶I
◀ | ▶
Back | Close
Full Screen / Esc
Printer-friendly Version
Interactive Discussion

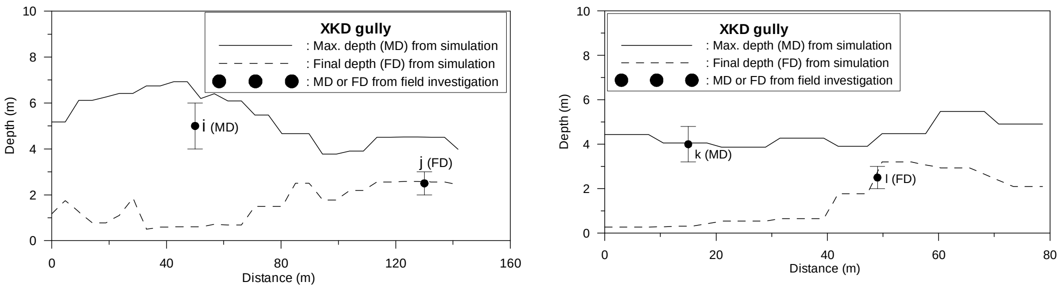

(a) section X1 (b) section X2

Fig. 8. Depths of the debris-flow profiles from the simulation compared to the depths from the field investigation of the XKD gully.

NHESSD
2, 315–346, 2014

Discharge of landslide-induced debris flows

J.-C. Chen and M.-R. Chuang

Title Page
Abstract | Introduction
Conclusions | References
Tables | Figures
◀| |▶
◀ ▶
Back | Close
Full Screen / Esc
Printer-friendly Version
Interactive Discussion

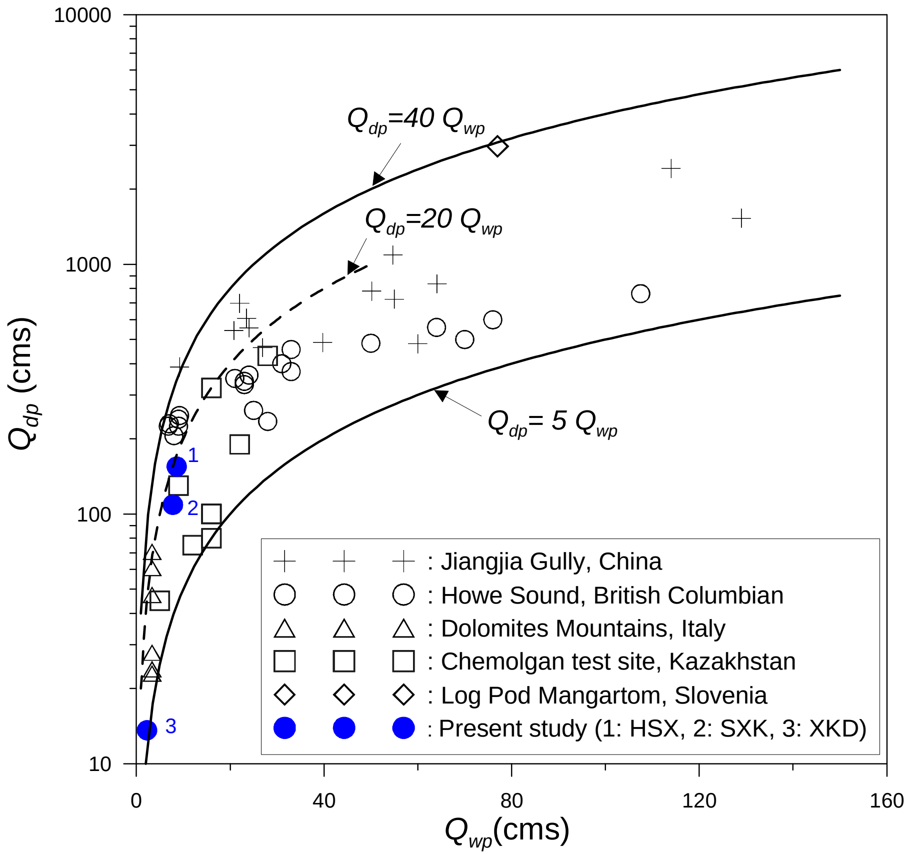

Fig. 9. Relationship between the debris-flow discharge Q_{dp} and the water-flow discharge Q_{wp}.

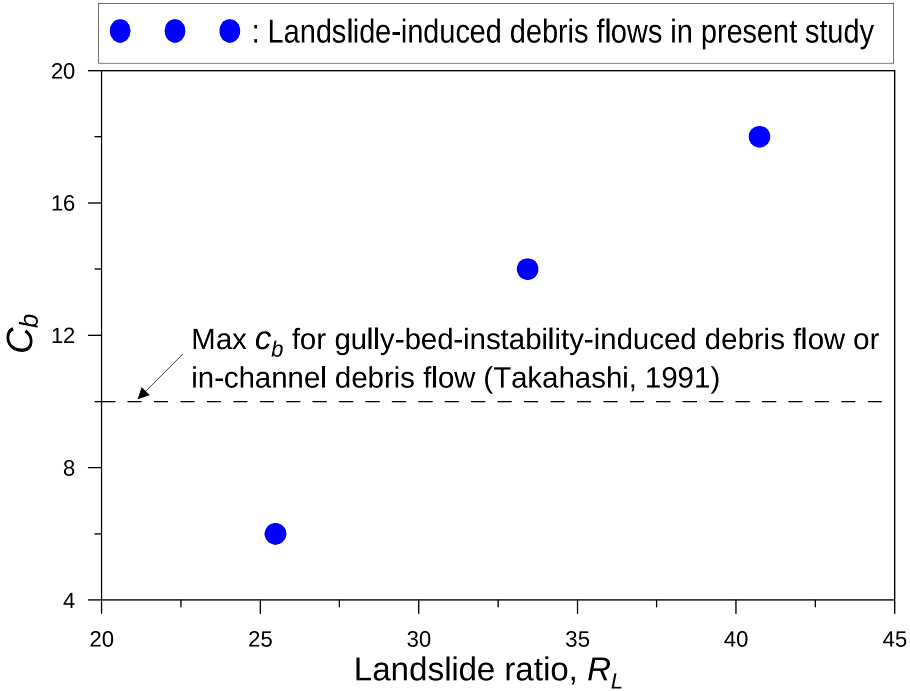

Fig. 10. Relationship between the discharge coefficient c_b and the landslide ratio R_L.